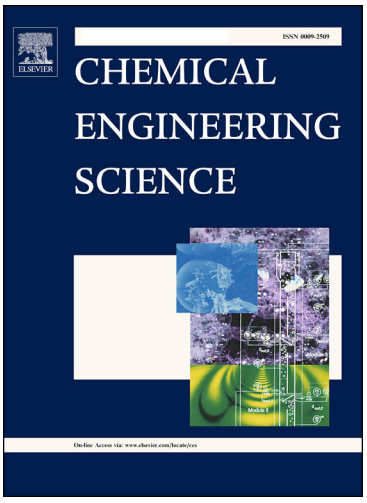

Non-spherical solid-non-Newtonian liquid fluidization and ANN modelling: minimum fluidization velocity

Samit Bikas Maiti, Sudipta Let, Nirjhar Bar, Sudip Kumar Das

PII: S0009-2509(17)30666-8
DOI: https://doi.org/10.1016/j.ces.2017.10.050
Reference: CES 13882

To appear in: *Chemical Engineering Science*

Received Date: 28 July 2017
Revised Date: 1 October 2017
Accepted Date: 29 October 2017

Please cite this article as: S. Bikas Maiti, S. Let, N. Bar, S. Kumar Das, Non-spherical solid-non-Newtonian liquid fluidization and ANN modelling: minimum fluidization velocity, *Chemical Engineering Science* (2017), doi: https://doi.org/10.1016/j.ces.2017.10.050

Non-spherical solid-non-Newtonian liquid fluidization and ANN modelling: minimum fluidization velocity

Samit Bikas Maiti, Sudipta Let, Nirjhar Bar and Sudip Kumar Das
Department of Chemical Engineering, University of Calcutta
92, A. P. C. Road, Kolkata – 700 009, India.
E-mail: drsudipkdas@vsnl.net

ABSTRACT

Experiments have been carried out to determine the minimum fluidization velocity for sand particles of irregular shape and size using pseudoplastic liquids in different Perspex columns. The effect of different operating parameters, like column diameter, particle size and shape, rheological properties of the liquid on minimum fluidization velocity has been investigated. It has been observed that as sphericity of the particle decreases, minimum fluidization also decreases. Empirical correlation has been developed to predict the minimum fluidization velocity as a function of physical and dynamic variable of the system. Statistical analysis of the correlation suggests that is of acceptable accuracy. Applicability of the artificial neural network modelling using gradient descent and Levenberg-Marquardt algorithm have also been successfully tested.

Keywords: minimum fluidization velocity, non-Newtonian liquid, sphericity, Levenberg-Marquardt algorithm

1. Introduction

Liquid fluidization is used in food processing, hydrometallurgy, biochemical processing, water treatment etc. The unit operations that utilize the fluidization technology are coal combustion, cracking, reforming in refinery, Fisher Tropsch synthesis, gasification, coking etc. The advantages of this technique is the ability to perform number of unit operation like heat and mass transfer, leaching, drying, mixing, segregation, granulating etc. When liquid is passed

through a fixed bed containing solid particle at low flow rate, then it passes through the voidages of the solid without disturbing the bed status. On increase in liquid velocity initially the bed particles start to expand, and then the upward drag force become equal to the downward forces, i.e. bed weight, this state is called incipient fluidization and the fluid velocity is known as minimum fluidization velocity. With further increase in liquid velocity the bed particle will expand and the condition is called fully fluidized condition (Richardson, 1971). The hydrodynamic characteristics of Newtonian fluids flowing through fixed and fluidized bed have been extensively studied and large number literatures are available (Richardson, 1971; Joshi, 1983; Kuni and Levenspiel, 1990; di Felice, 1995; Jamialahmadi and Müller-Steinhagen, 2000). Couderc (1985) has critically examined the existing literature and concluded that value of minimum fluidization velocity for Newtonian medium can be estimated accurately (with an average error of 10-15%) for all practical cases.

Non-Newtonian liquids are used in a wide variety of industrial applications. Non-Newtonian liquids are extensively used in chemical, petroleum, petrochemical, mineral processing industries, bubble columns, polymer solution and food industries (Das et al., 1989, Chhabra, 1993). Availability of literature on pseudoplastic liquid flow through fluidized bed is very less compare to that of Newton liquid flow system (Chhabra, 1993). Srinivas and Chhabra (1991) critically reviewed the non-Newtonian pseudoplastic flow through the fluidized bed on spherical particles. Sharma and Chhabra (1992) reported the non-Newtonian liquid flow through fixed and fluidized bed using non-spherical particles. Chhabra (1993) examined all the correlations available and concluded that the estimation of the minimum fluidization velocity for non-Newtonian liquids is difficult. Chhabra et al. (2001) and Chhabra (1993) reviewed all the existing literature on the non-Newtonian liquid-solid fluidization. Literature review suggested

that the following two approaches are used to predict the minimum fluidization velocity for non-Newtonian liquid-spherical particle. The approaches are presented in the following equations,

$$Ar = f_1\left(n, \varepsilon_{mf}\right)\mathrm{Re}_{mf}^{2/(2-n)} + f_2\left(n, \varepsilon_{mf}\right)\mathrm{Re}_{mf}^{2/(2-n)} \quad (1)$$

and

$$\frac{V_{mf}}{V_t} = f\left(\varepsilon_{mf}, n, \mathrm{Re}_t\right) \quad (2)$$

Different researchers have defined f_1 and f_2 to fit their own data (Yu et al., 1968; Mishra et al., 1975; Brea et al., 1976; Kumar and Upadhyay, 1981; Kawase and Ulbrecht, 1985; Jaiswal et al. 1992). Chhabra (1993) and Chhabra et al. (2001) concluded that for the minimum fluidization velocity predict the average error as 20-25% and for creeping flow region it is more than 60% for polymer solution and more than 100% for suspension. Whereas for Eq (2), the average error is more (Machač et al., 1986; Machač et al., 1993; Machač et al. 2005). Aghajani et al. (2004) compared the experimental and published data from the literature for the hydrodynamic parameters of fluidized beds for solid-Newtonian and solid-non-Newtonian systems. Broniarz-Press et al. (2007) reported the experimental result on the effect of properties of the liquid on the resistance of flow through fluidized beds. For the solid-non-Newtonian liquid fluidization only few experimental data are available for non-spherical particles. Chhabra et al. (2001) reported that by applying both approaches for non-spherical particle yield large deviation, hence it has very limited application.

The use of Artificial Neural Network (ANN) are extremely useful for generalization purpose in recent years and it is clear from the large number of publications that is available in various field like engineering, scientific, climate science, economic, finance etc. The advantages of ANN are clearly demonstrated in literature (Bar et al., 2010a, b). From the survey of literature

it is clear that the use of ANN yields satisfactory results related to input and output mapping without any knowledge of the interim states/steps of algorithm used, i.e., in cases where it becomes difficult to find mathematical relationships between the parameters (Lippman, 1987; Himmelblau, 2000; Pirdashti et al. 2013). Recently, a number of software's (Matlab, R, Statistica, Neurosolution etc.) are available in the market which can be used for ANN analysis in dealing with many complex problems.

ANNs are used as tools for analyzing complex relationships in complex systems within a big framework. If it is trained with small dataset then the unstable behavior in the performance may be observed (Bowden 2002). But now-a-days researchers are able to handle small datasets either experimental or observational data through ANNs for modelling (Forman and Cohen, 2004; Herzag, 2006; Bar et al., 2010a; Pasini, 2015; Shaikhina and Khovanova, 2017). The present paper deals with the experimental determination of minimum fluidization velocity using pseudoplastic non-Newtonian liquids and non-spherical particles. An empirical correlation and the artificial neural network modelling has been used for the prediction of minimum fluidization velocity.

2. Experimental

Fig.1 represents the schematic diagram of experimental setup. It consists of liquid storage tank, liquid distribution section, flow rate and measuring devices. The fluidization column is made of Perspex and has an internal diameter of 92.3 mm, 72.0 mm and 47.0 mm and height 1376.2 mm. The entire test section is vertically mountain to prevent vibration. The lower part is the liquid distribution section filled with the glass marbles of the size ranging from 1–3 cm in diameter for uniform distribution of liquid in the column. The marbles are supported and enclosed by 16 mesh stainless steel grid. Pressure trappings are provided to measure pressure

drop of the column. Simple U-tube and/or inclined manometers containing mercury beneath the water are used for the measurement for pressure difference across the column. Arrangement of purging the solution in manometer line is also provided. Initially experiments have been carried out using water to test the apparatus. A scale is fitted on the outer surface of the column to measure the bed height.

A rectangular tank (0.45 m^3) is used for storage of liquid and is fitted with propeller type stirrer for uniform mixing of sodium salt of carboxymethyl cellulose (SCMC) (high viscous grade, Loba Chemie Pvt. Ltd., Mumbai, India). Required amount of SCMC has been dissolved in tap water by stirring to form homogeneous solution and kept for more than 15 hours for ageing. Trace amount of formaldehyde has been added to prevent biodegradation. The liquid is kept at constant temperature by recirculation of tap water through a copper coils. A centrifugal pump is used to circulate the liquid from the tank. Rotameter RL1 [Transducer and Controls Pvt. Ltd., Hyderabad, India, accuracy ±2%] has been used to measure the flow rate and is controlled by a bypass valve. The liquid discharge from the test section is returned to the tank. The liquid flow rate is also measure by collecting the liquid in certain interval of time at the discharge point.

Sand particles of different sizes are used as solid particles in the fluidised bed. The size and properties of the sand are given in Table 1. Dilute aqueous solutions of Sodium salt of carboxyl methyl cellulose (SCMC) is used as non-Newtonian pseudoplastic liquid. Rheological properties have been measured in pipeline viscometer and other physical properties have been measured using conventional technique. Table 2 shows the rheological and other physical properties of the liquids. The sphericity of sand particle is measured by permeability test applying the Kozeny-Carman equation (Carman, 1956). Dilute solution of SCMC is a pseudoplastic time independent liquid and follow the power law model as

$$\tau = K\left(\frac{dU}{dr}\right)^{n} \tag{3}$$

In general, shear thinning pseudoplastic liquid calculations are carried out on the basis of effective viscosity (μ_{eff}), as (Das et al. 1989),

$$\mu_{eff} = 8^{n'-1} D^{1-n'} U_l^{n'-1} K' \tag{4}$$

Where, $n = n'$ and $K' = K\left(\frac{3n'+1}{4n'}\right)^{n'}$

In actual experiment, first measured quantity of sand has been introduced in the column. The experimental liquid is introduced into the test section by means of pump and then its flow rate has been controlled using bypass valve. The pressure drop across the bed has been measured using manometer. The extent of bed expansion is estimated from the knowledge of the initial height of the bed and the expanded bed height is measured simply with the help of graduated scale fixed in the column. For each size of particles, the experiment is repeated number of times to ensure the reproducibility of the data. The flow order of the experimental run is determined by lot to avoid systematic error. The minimum fluidization velocity has been estimated from the intersection of pressure drop flow rate plots in the fixed and fluidised bed regimes.

3. ANN modeling

Fig. 2 presents the schematic diagram of ANN used. Considering the popularity of the structure of ANN, a three-layered MLP (Multilayer perceptron) is used for the proposed modelling (Lippman, 1987). However, depending upon the success of the proposed modelling this structure is liable to change. The proposed modelling has also being developed using Neurosolution 5.07 software, four well-known transfer functions (TF I — TF IV) and two well-known algorithms, i.e., gradient descent and Levenberg-Marquardt.

4. Result and discussion

4.1 Minimum fluidization velocity determination

The minimum fluidization is defined as the lowest superficial velocity at which downward forces become equal to the upward drag force. The actual pressure drop, ΔP, has been measured for a liquid velocity, U_l, by subtracting the solid-free pressure drop, ΔP_o, from the observed pressure drop, ΔP_a, in presence of solid. Hence

$$\Delta P = \Delta P_a - \Delta P_o \tag{5}$$

In solid-liquid fluidization, minimum fluidization velocity is determined from the plot of pressure drop across the bed versus the liquid velocity as shown in Fig. 3. The figure indicates that the pressure drop increases with velocity (A→B) and ultimately reaches a constant pressure drop zone (B→C). This (A→B) zone is called static bed zone. The (B→C) zone is the fluidised bed zone. The point of intersection of the increasing part of the curve and the constant region represents the minimum fluidization velocity.

4.2 Effect of different parameters on the minimum fluidization velocity

The plot of ΔP versus U_l for different system are shown in Figs. 4–6. Fig. 4 indicates that as the particle diameter increases, the minimum fluidization velocity also increases at constant tube diameter and SCMC concentration. The Fig. 5 shows the variation of minimum fluidization velocity with the SCMC solution concentration and it is observed that U_{mf} decreases with an increase in SCMC concentration. The decrease of minimum fluidization velocity is due to decrease in Archimedes number with the increase in viscous force resulting from the increase of liquid viscosity, i.e., pseudoplasticity increases with increase in SCMC concentration. Fig. 6 shows the variation of column diameter on the minimum fluidization velocity and Fig. 7 indicates the variation of minimum fluidization velocity with the column diameter and both

figures indicates that the minimum fluidization velocity is independent of column diameter. Wicke and Hedden (1952) pointed out that if the ratio of $d_c/d_p \geq 10$ the wall effect is negligible for fluidization. In the present case this ratio is much higher hence there is no wall effect on the fluidization.

At the minimum fluidization condition the particles are away from each other and move in upward direction due to fluid velocity. As particles move in upward direction, the fluid just above the particles moves in the downward direction from all sides. This upward and downward motion of the fluid across the particle effectively reduces the fluid velocity in the vicinity of the particles and is applicable throughout the bed. Hence, pseudoplasticity of the liquid increases in the vicinity of the solid particles, thus the viscosity also increases and hence minimum fluidization velocity decreases. As the sphericity of the particle decreases the fluid motion in downward direction is more compared to that of the spherical particle, i.e., $\phi = 1$. Pittyjohn and Christiansen (1948) observed that the particles of lower sphericity reduces the settling velocity so increases the minimum fluidization velocity and it is only true for solid-Newtonian fluids system.

4.3 Empirical correlation for minimum fluidization velocity

The minimum fluidization velocity, U_{mf}, in liquid-solid fluidised beds is a function of physical and dynamic variables of the system. The following factors affect the minimum fluidization velocity,

1. Diameter: particle, d_p and the column, d_c
2. Physical properties of the liquid: viscosity, μ_{eff}, density, ρ_l
3. Physical properties of the solid: density ρ_p and sphericity, ϕ
4. Acceleration due to gravity: g

Hence, the minimum fluidization velocity can be expressed as,

$$U_{mf} = f\left(d_p, d_c, \mu_{eff}, \rho_s, \rho_l, \phi, g\right) \tag{6}$$

The use of dimensional analysis the above functional relationship can be reduced to the following functional relationship (combining the variable),

$$\mathrm{Re}_{mf} = f\left(Ar, \frac{d_c}{d_p}, \phi\right) \tag{7}$$

The multiple linear regression (MLR) analysis suggested the following correlation,

$$\mathrm{Re}_{mf} = 0.0204 Ar^{0.905\pm0.0494} \left(\frac{d_c}{d_p}\right)^{0.589\pm0.091} \phi^{1.300\pm0.332} \tag{8}$$

For, $0.00071 \le \mathrm{Re}_{mf} \le 1.02297$

$0.0012 \le Ar \le 23.8925$

$23.15271 \le (d_c/d_p) \le 171.5613$

$0.5015 \le \phi \le 0.7965$

The value of Re_{mf} as predicted by Eq. (8) have been plotted against the experimental values as shown in Fig. 8. The correlation coefficient and the variance of estimate of the above equation are 0.9856 and 0.0336 respectively, for a **t** value of 2.00 for 50 degree of freedom at 0.05 probability level and 95% confidence range (Volk, 1958).

4.4 ANN performance

The analysis is performed using gradient descent (GD) and Levenberg Marquardt (LM) training algorithms. Table 3 gives the range of data for ANN analysis. For the hidden layer of the GD network the value of learning rate (α) is 0.7 and that of momentum coefficient (μ) is 1. The input variables are n', K', density of liquid, ρ_l, sphericity of particle, ϕ, particle diameter, d_p and

column diameter, d_c. The output variable is the minimum fluidization velocity, U_{mf}. There is a total of 54 data points.

The parameter for optimization has been the minimum cross-validation MSE value reached during training and is represented in Table 4. The optimum number of hidden layer nodes corresponding to the respective transfer functions (TF's) is also listed in Table 5. These optimum numbers of nodes of the hidden layer is used for final analysis. Fig. 9 shows the variation of minimum value of cross-validation MSE with the number of epochs for the LM algorithms. The same process applied for the training with GD algorithm.

Fig. 10 represents the cross-validation curve for training with the GD algorithm. From the curve the minimum MSE can be seen at the maximum allotted 32000 epochs for TFs I, III and IV. For TF II it can be said that the cross-validation MSE reaches its minimum before 32000 epoch mark. However, the limitation of the software (Neurosolution 5.07) cannot permit the training to continue beyond 32000 epochs.

Fig. 11 represents the cross-validation curve for analysis with the LM algorithm. From the curve the minimum MSE's are observed. From the Fig. 11 it can be observed that for TF I to TF IV the horizontal straight line indicates non-improvement of MSE value for 100 consecutive epochs. The abrupt stopping of training for all the transfer functions can be observed before reaching the allotted 1000 epoch as scheduled. In this case the stopping criterion has been based on the improved capacity of the training within 100 epochs. For all the cases the training stopped due to the application of stopping criterion.

Table 5 presents the values of AARE, SD, MSE and cross-correlation coefficient (R) related to the analysis for final prediction. Table 5 also confirms the excellent result, i.e., the closeness of data. The closeness of data demands χ^2 test for drawing conclusion. The χ^2 test

confirms that the transfer function 4 with 7 processing elements (optimum number) give the best result using LM algorithm. The excellent correlation is evident from the Fig. 12, which is the plot between experimental and predicted values of minimum fluidization velocity.

Considering the extremely low values, i.e., 0.005155 for AARE, 0.003659 for SD, 1.59×10^{-8} for MSE and also the *R* value of 0.999968 suggest that the proposed ANN modelling have been very successful. Therefore, the success of this ANN modelling negates the thought of restructuring this proposed ANN structure.

4.5 Comparison of the different method

Chhabra (1993) compared the available correlations (Yu et al., 1968; Mishra et al., 1975; Brea et al., 1976; Kumar and Upadhyay, 1981; Kawase and Ulbrecht, 1985; Jaiswal et al., 1992; Machač et al., 1993) and presented high absolute mean average error (28 – 58%). This result was unacceptable. Table 6 presents the absolute mean average error for the minimum fluidization velocity by different correlation. The absolute mean average error is defined as

$$AE = \frac{1}{N}\sum \left| U_{mf,Expt} - U_{mf,Cal} \right| X 100\% \tag{9}$$

The conventional model, i.e., multiple linear regression, is to recognize parameters that affect the object parameter, whereas in ANN models, the possible interpretation of relationships between parameters are not possible. Model performance has been assessed by using correlation coefficient. The correlation coefficient for MLR model and best ANN model are 0.9856 and 0.999968 respectively and the ANN model also gives the minimum deviation (Table 6). Hence ANN model has slightly higher prediction accuracy. Similar results are also obtained in the different fields of ANN application (Baker and Richards, 1999; Elhag et al., 2006; Herzag, 2006; Bandyopadhyay and Chottapadhyay, 2007, Youn and Gu, 2010; Thongboonnak and Sarapirome, 2011; Laxmi and Kumar, 2011; Ayooubi and Sahrawat, 2011; Mehnatkesh et al., 2012, Shi et al.,

2013; Tosun, et al., 2016, Heddam, 2016). Youn and Gu (2010) reported that ANN gives better accuracy than linear regression for small dataset.

5. Conclusion

The hydrodynamic characteristics of normal fluidised bed have been experimentally investigated and fluidization with non-Newtonian pseudoplastic liquids using sand has been studied. The minimum fluidization velocity increases with the increase in particle diameter but decreases with increase in the pseudoplasticity of the liquid. It is independent of the column diameter. It decreases with decrease in the sphericity of the sand particle. Empirical correlation has been developed to predict the minimum fluidization velocity as a function of physical and dynamic variables of the system. Statistical analysis suggests that the correlation is of acceptable accuracy. Successful ANN modelling has also been established.

Acknowledgement

Mr. Samit B. Maiti is thankful for the non-gate fellowship, UGC, Govt of India and Mr. Sudipta Let is thankful to UGC, Govt. of India for RGNF research fellowship.

Nomenclature

d, D	diameter, m
g	acceleration due to gravity, m/s^2
K, K'	consistency index (N s n$'$/m^2)
n, n'	flow behavior index
N	number of data points
r	radius, m

R correlation coefficient, $R = \dfrac{\sum_{i=1}^{N}(x_i - \bar{x})(y_i - \bar{y})}{\sqrt{\sum_{i=1}^{N}(x_i - \bar{x})^2 \sum_{i=1}^{N}(y_i - \bar{y})^2}}$, dimensionless

U velocity, m/s

Ar Archimedes No. $Ar = \dfrac{d_p^3 g\left(\rho_p - \rho_l\right)}{\mu_{eff}^2}$, dimensionless

Re particle Reynolds No. $\mathrm{Re} = \dfrac{U_l d_p \rho_l}{\mu_{eff}}$, dimensionless

TF I Transfer function 1, $f_{1h}(x) = \tanh \beta x = \dfrac{e^{\beta x} - e^{-\beta x}}{e^{\beta x} + e^{-\beta x}}$, dimensionless

TF II Transfer function 2, $f_{2h}(x) = \beta x$ Where $\begin{matrix} \beta x = 1 \text{ for } \beta x > 1 \\ \beta x = -1 \text{ for } \beta x < -1 \end{matrix}$, dimensionless

TF III Transfer function 3, $f_{3h}(x) = \beta x$ Where $\begin{matrix} \beta x = 0 \text{ for } \beta x < 0 \\ \beta x = 1 \text{ for } \beta x > 1 \end{matrix}$, dimensionless

TF IV Transfer function 4, $f_{4h}(x) = \dfrac{1}{1 + e^{-\beta x}}$, dimensionless

MSE Mean Squared Error, $\frac{1}{N}\sum_{i=1}^{N}\left(x_i - y_i\right)^2$, dimensionless

AARE Average Absolute Relative Error $AARE = \frac{1}{N}\sum_{i=1}^{N}\left|\dfrac{\left(y_i - x_i\right)}{x_i}\right|$, dimensionless

Greek letters

α learning rate in GD algorithm

ε voidage, dimensionless

ρ density, kg/m^3

ϕ Sphericity of the particle, dimensionless

μ viscosity, kg-m/s

μ momentum coefficient in GD algorithm

χ^2 $\chi^2 = \sum_{i=1}^{N} \frac{(x_i - y_i)^2}{y_i}$, dimensionless

σ $\sigma = \sqrt{\sum_{i=1}^{N} \frac{1}{N-1} \left[\left| \frac{(y_i - x_i)}{x_i} \right| - AARE \right]^2}$, dimensionless

ΔP pressure drop, N/m^2

Subscript

a with solid

c column

i species

l liquid

o solid free

p particle

t terminal velocity

mf minimum fluidization

eff effective

References

Aghajani, M., Müller-Steinhagen, H., Jamialahmadi, M., 2004. Experimental Results and Models for Solid/Liquid Fluidized Beds Involving Newtonian and Non-Newtonian Liquids. Dev. Chem. Eng. Mineral Process 12(3-4), 403–426.

Ayoubi, S., Sahrawat, K. L., 2011. Comparing multivariate regression and artificial neural network to predict barley production from soil characteristics in northern Iran. Archives Agronomy and Soil Sci. 57(5), 549–565.

Baker, B., Richards, C.E., 1999. A comparison of conventional linear regression methods and neural networks for forecasting educational spending. Eco. Edu. Review, 18, 405-415.

Bandyopadhyay, G., Chattopadhyay, S., 2007. Single hidden layer artificial neural network models versus multiple linear regression model in forecasting the time series of total ozone. Int J. Environ. Sci. Technol., 4(1) 141-149.

Bar, N., Bandyopadhyay, T. K., Biswas, M. N., Das, S. K., 2010a. Prediction of pressure drop using artificial neural network for non-newtonian liquid flow through piping components J. Pet. Sci. Engg., 71(2-3), 187-194.

Bar, N., Biswas, M. N., Das, S. K., 2010b. Prediction of pressure drop using artificial neural network for gas non-newtonian liquid flow through piping components Ind. Engg. Chem. Res., 49(19), 9423–9429.

Bowden, G. J., Maier, H. R., Dandy, G. C., 2002. Optimal division of data for neural network models in water resources applications. Water Resour. Res., 38(2), 1-11.

Brea, F.M., Edwards, M.F., Wilkinson W. L., 1976. The flow of non-Newtonian slurries through fixed and fluidized beds. Chem. Eng. Sci. 31, 329–336.

Broniarz-Press, L., Agacinski, P., Rozanski, J., 2007. Shear-thinning fluids flow in fixed and fluidized beds. Int. J. Multiphase Flow 33(6), 675–689.

Carman, P.C., 1956. Flow of gases through porous medium. Ch. IV, Butterworths, London.

Chhabra,R.P., 1993. Bubbles, drops, and particles in non-Newtonian fluids. Boca Raton, CRC Press.

Chhabra R.P., 1993. Estimation of the minimum fluidization velocity for beds of spherical particles fluidized by power law liquids. Powder Technol. 76, 225–228.

Chhabra, R.P., Comiti J., Machač, I., 2001. Flow of non-Newtonian fluids in fixed and fluidized beds. Chem. Eng. Sci. 56, 1–27.

Couderc, J.P., 1985. Fluidization, Eds. J. F. Davidson, D. Clift, D. Harrison, Academic Press, New York, 2nd Ed.

Das, S.K., Biswas, M.N., Mitra, A.K. 1989. Pressure losses in two-phase gas-non-Newtonian liquid flow in horizontal tube. J. Pipelines **7**, 307–325.

di Felice, R., 1995. Hydrodynamics of liquid fluidisation. Chem. Engg. Sci. 50, 1213–1245.

Elhag, T., Wang, Y-M., Ballal, T., 2006. Managing highways maintenance projects: neural networks vs. regression techniques. Proc. Joint Int. Conf. Construction, Culture, Innovation and Mang. (CCIM) Dubai, UAE, Jan. 1, 2006, 535-542.

Forman, C., Cohen, I., 2004. Learning from little : comparison of classifiers given little training. Proc. PKDD, 19, 161-172.

Heddam, S., 2016. Secchi disk depth estimation from water quality parameters: artificial neural network versus multiple linear regression models?. Environ. Process. 3, 525-536.

Herzag, S., 2006. Estimating students retention and degree completion time : decision trees and neural networks vis-à-vis regression. New Directions for Institutional Research., 2006(131), 17-33.

Himmelblau, D.M., 2000. Applications of artificial neural networks in chemical engineering. Korean J. Chem. Eng. 17(4), 373–392.

Jaiswal, A.K., Sundararajan, T., Chhabra, R.P., 1992. Simulation of non-Newtonian fluid through fixed and fluidized beds of spherical particles. Numerical Heat Transfer 21(3), 275–297.

Jamialahmadi, M., Müller-Steinhagen ,H., 2000. Hydrodynamics and heat transfer of liquid fluidized bed systems. Chem. Engg. Comm. 179, 35–79.

Joshi,J.B., 1983. Solid-liquid fluidized beds: some design aspects. Chem. Engg. Res. Des. 61, 143–161.

Kawase, Y., Ulbrecht, J., 1985. Mass and momentum transfer with non-Newtonian fluids in fluidized beds. Chem. Engg. Commun. 32(1-5), 263–288.

Kumar, S., Upadhyay S.N., 1981. Mass and momentum transfer to Newtonian and non-Newtonian fluids in fixed and fluidized beds. Ind. Engg. Chem. Res. 20(3), 186–195.

Kuni, D., Levenspiel, O., 1990. Fluidisation Engineering, Second Edition, Stoneham, MA: Butterworths, 1990.

Laxmi, R. R., Kumar, A., 2011. Weather based forecasting for crops yield using neural network approach Statistics and Application. 9(1-2) 55–59.

Lippman, R., 1987. An introduction to computing with neural nets. IEEE ASSP Mag. 4(2), 4–22.

Machač, I., Balcar, M., Lecjaks, Z., 1986. Creeping flow of non-Newtonian liquids through fluidized beds of spherical particles. Chem. Eng. Sci. 41(3), 591–596.

Machač, I., Mikulášek, P., Ulbrichová, I., 1993. Non-Newtonian fluidization of spherical-particle beds. Chem. Engg. Sci. 48(11), 2109–2118.

Machač, I., Šiška, B., Machačová, L., 2005. Fluidization of spherical particle beds with non-Newtonian suspension. Chem. Biochem. Eng. Q. 19(2), 123–132.

Mehnatkesh, A., Ayoubi, Sh., Jalalian, A., Dehghani, A. A., 2012. Prediction of rainfed wheat grain yield and biomass using artificial neural networks and multiple linear regressions and determination the most factors by sensitivity analysis. CIGR-Ag-Eng 2012: International Conference of Agricultural Engineering. Valencia, Spain.

Mishra, P., Singh, D., Mishra, I.M., 1975. Momentum transfer to Newtonian and non-Newtonian fluids flowing through packed and fluidized beds. Chem. Eng. Sci. 30, 397–405.

Pasini, A., 2015. Artificial neural networks for small dataset analysis. J. Thorac. Dis., 2015. 7(5) 953-960.

Pirdashti, M., Curteanu, S., Kamangar, M.H., Hassim, M.H., Khatami, M.A., 2013. Artificial neural networks: applications in chemical engineering. Rev. Chem. Eng. 29(4), 205–239.

Pittyjohn, E.S., Christiansen, E.B., 1948. Effects of particle shape on free settling rates of isometric particles. Chem. Eng. Prog. 44(2),157–172.

Richardson, J.F., 1971. Incipient fluidization and particulate systems, In Fluidization, J. F. Davidson and D. Harrison (Eds.) Ch. 2, page 25, New York, Academic Press.

Shaikhina, T., Khovanova, N.A., 2017. Handling limited datasets with neural networks in medical applications: a small-data approach. Artificial Intell. Med., 75, 51-63.

Shi, H-Y., Lee, K-T., Lee, H-H., Ho, W-H., Sun, D-P., Wang, J-J., Chiu, C-C., 2012. Comparison of artificial neural network and logistic regression models for predicting in-hospital mortality after primary liver cancer surgery. PLoS One, 7(4), e35781.

Sharma, M.K., Chhabra R.P., 1992. An experimental study of non-Newtonian fluid flow through fixed and fluidized beds of non-spherical particles. Can. J. Chem. Eng. 70(3), 586–591.

Srinivas, B.K., Chhabra, R.P., 1991. An experimental study of non-Newtonian fluid flow in fluidized beds: minimum fluidization velocity and bed expansion characteristics. Chem. Engg. Process. 29(3), 121–131.

Thongboonnak, K., Sarapirome, S., 2011. Integration of Artificial Neural Network and Geographic Information System for Agricultural Yield Prediction. Suranaree J. Sci. Technol. 18(1), 71-80.

Tosun, E., Aydin, K., Bilgili, M, 2016. Comparison of linear regression and artificial neural network model of a diesel engine fueled with biodiesel-alcohol mixtures. Alexandria Engg. J., 55(4), 3081-3089.

Volk V., 1958. Applied statistic for engineers. McGraw-Hill Book Company, New York.

Wicke, E., Hedden, K., 1952. Strömungsformen und wärmeübertragung in von luft aufgewirbelten schüttgutschichten. Chem. Ing. Tech. 24(2), 82–91.

Youn, H., Gu. Z., 2010. Predicting Korean lodging firm failure : an artificial neural network model along with a logistic regression model. Int. J. Hospitality Mang., 29(1) 120-127.

Yu,Y.H., Wen, C.Y., Bailie, R.C., 1968. Power-law fluids flow through multiparticle system. Can. J. Chem. Eng. 46(3), 149–154.

LIST OF FIGURES

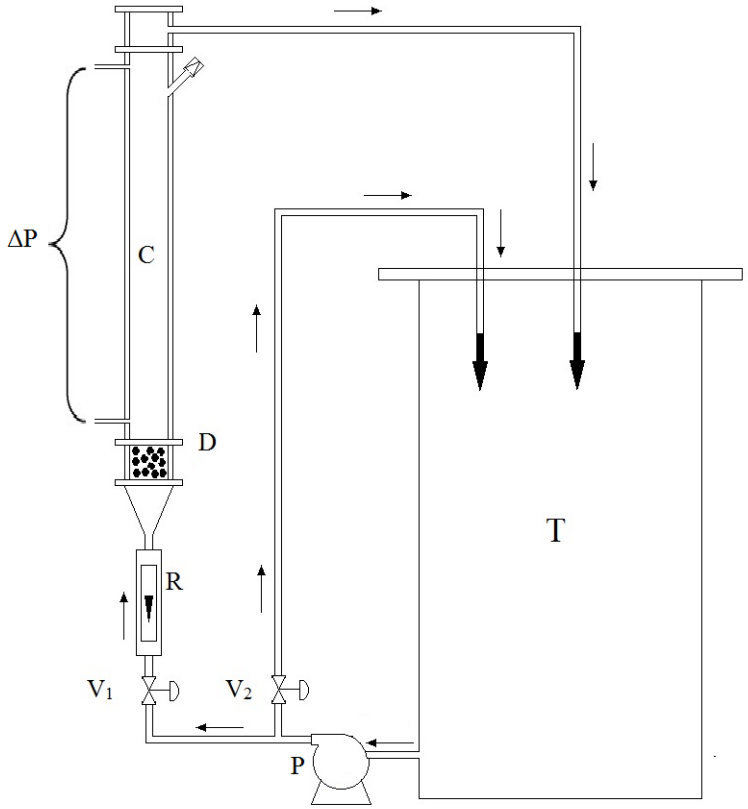

Figure 1

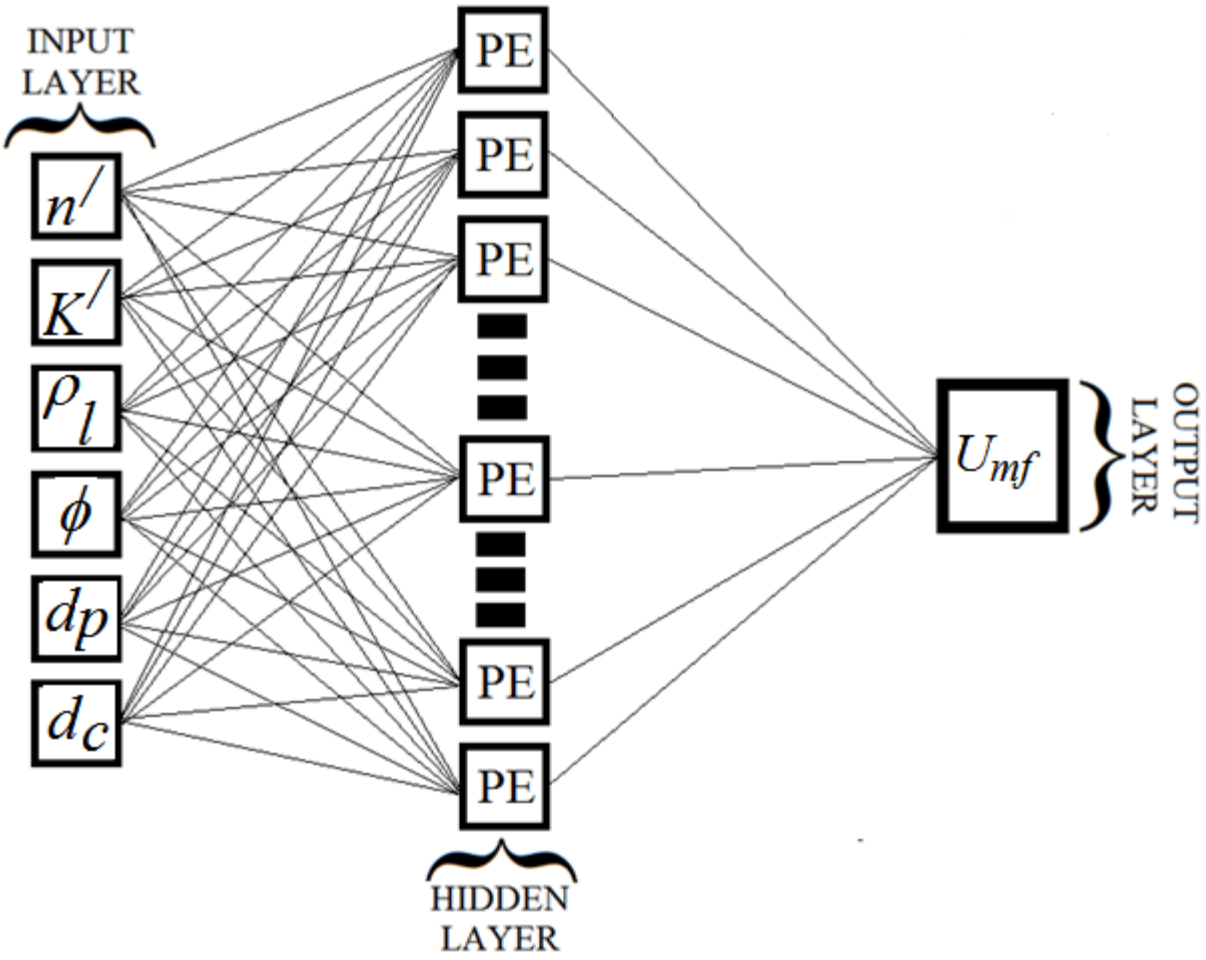

Figure 2

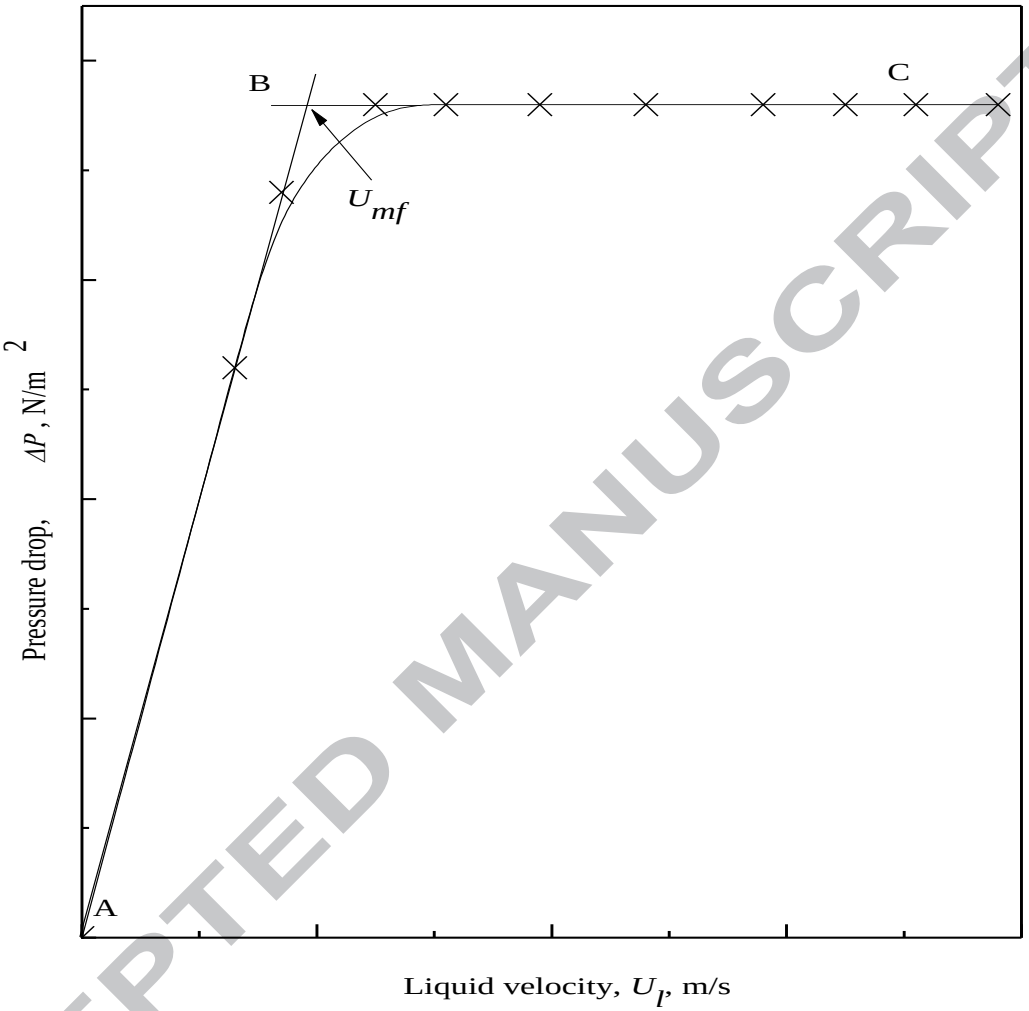

Figure 3

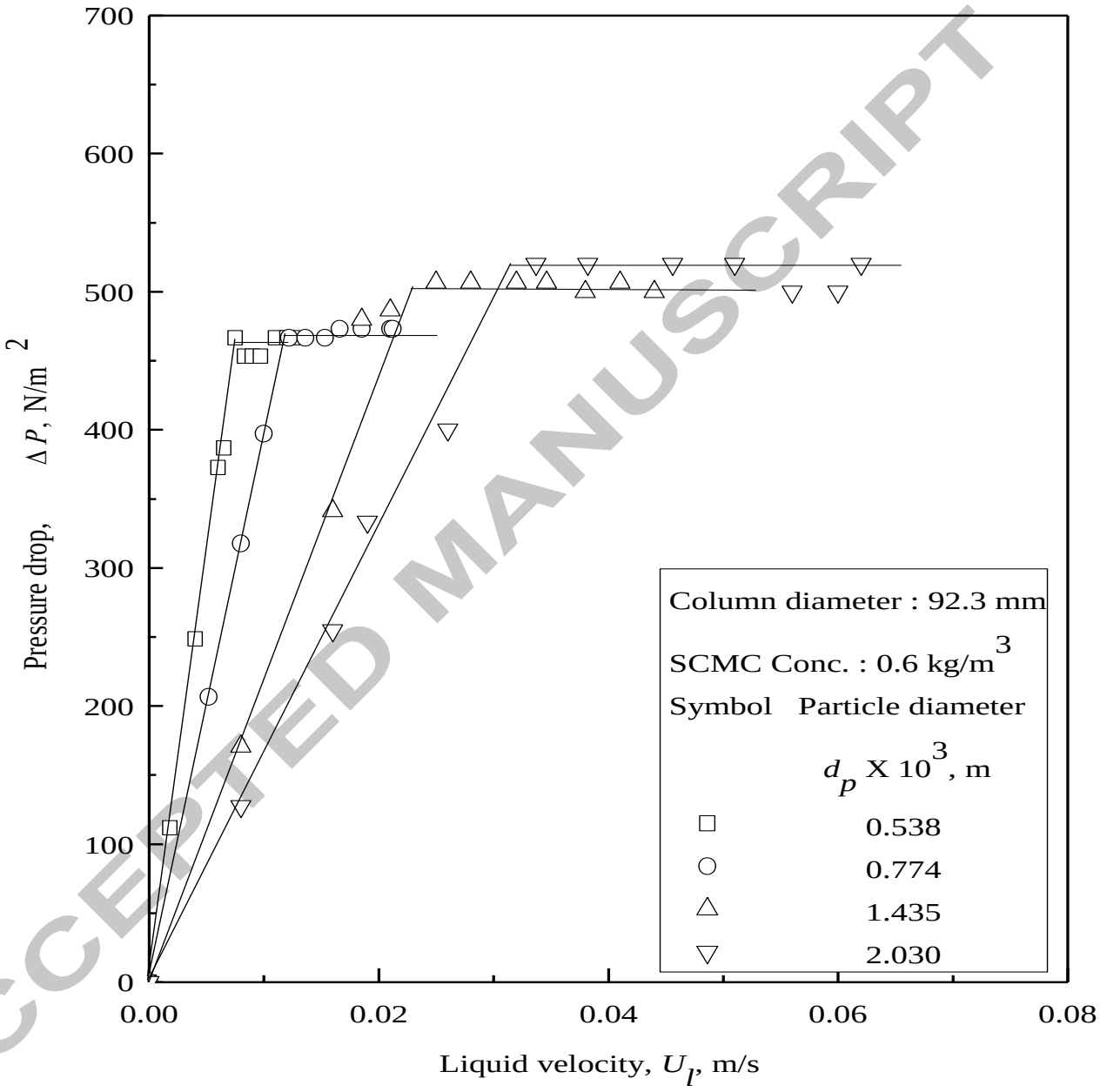

Figure 4

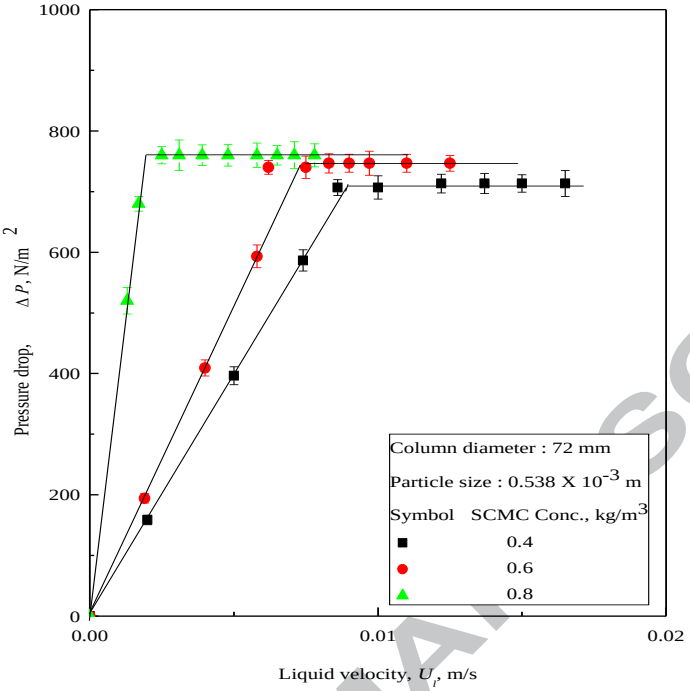

Figure 5

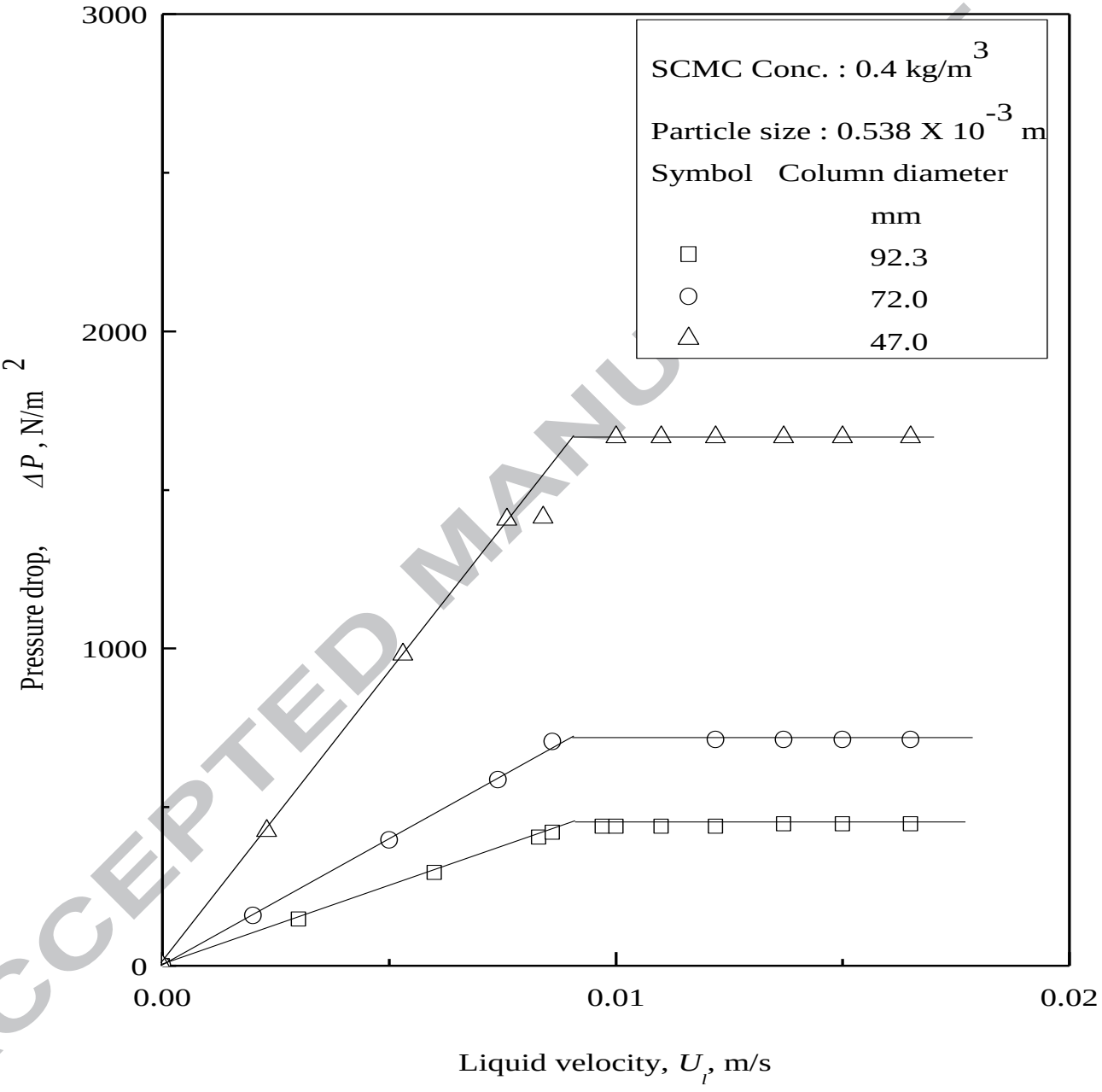

Figure 6

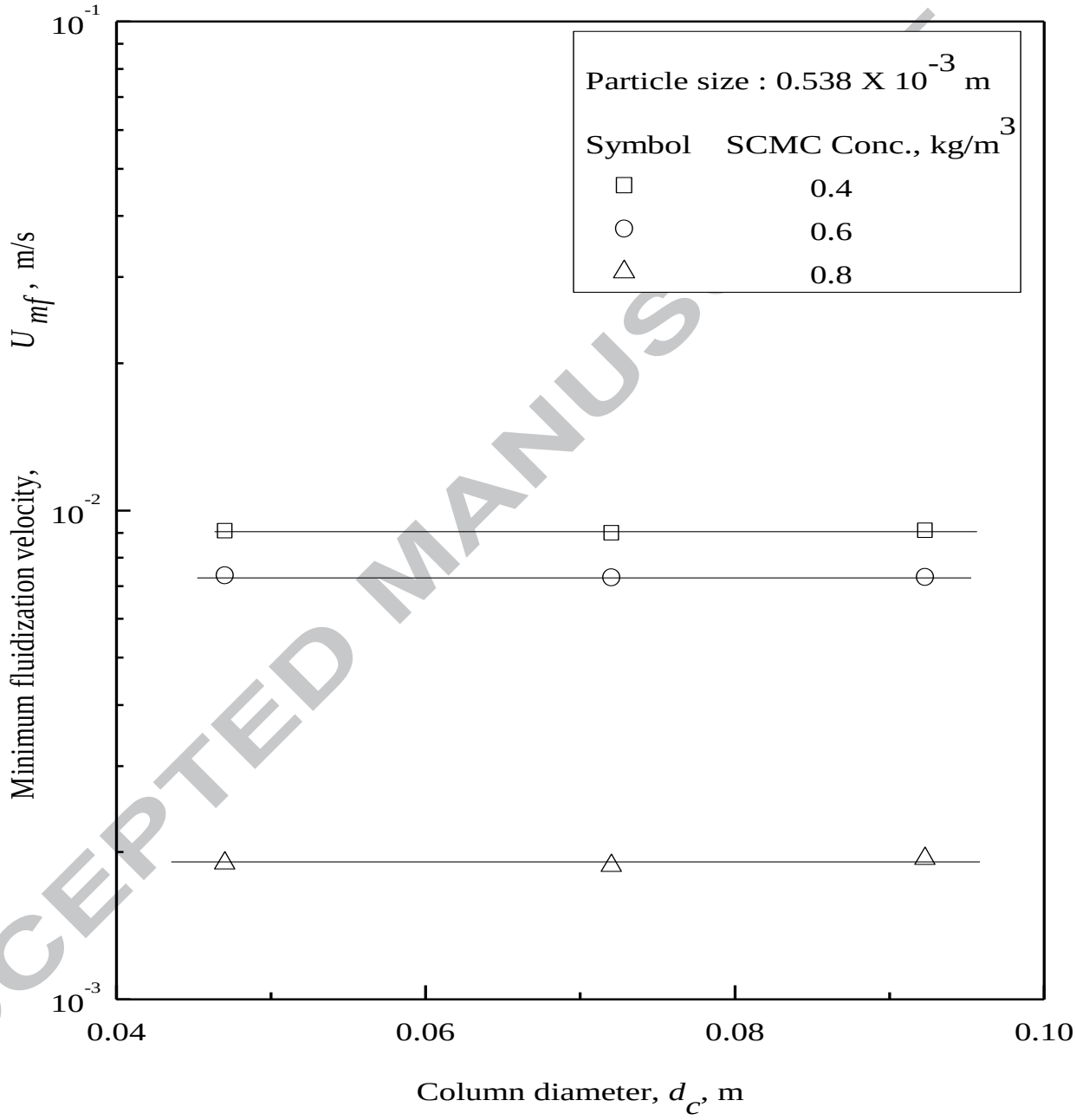

Figure 7

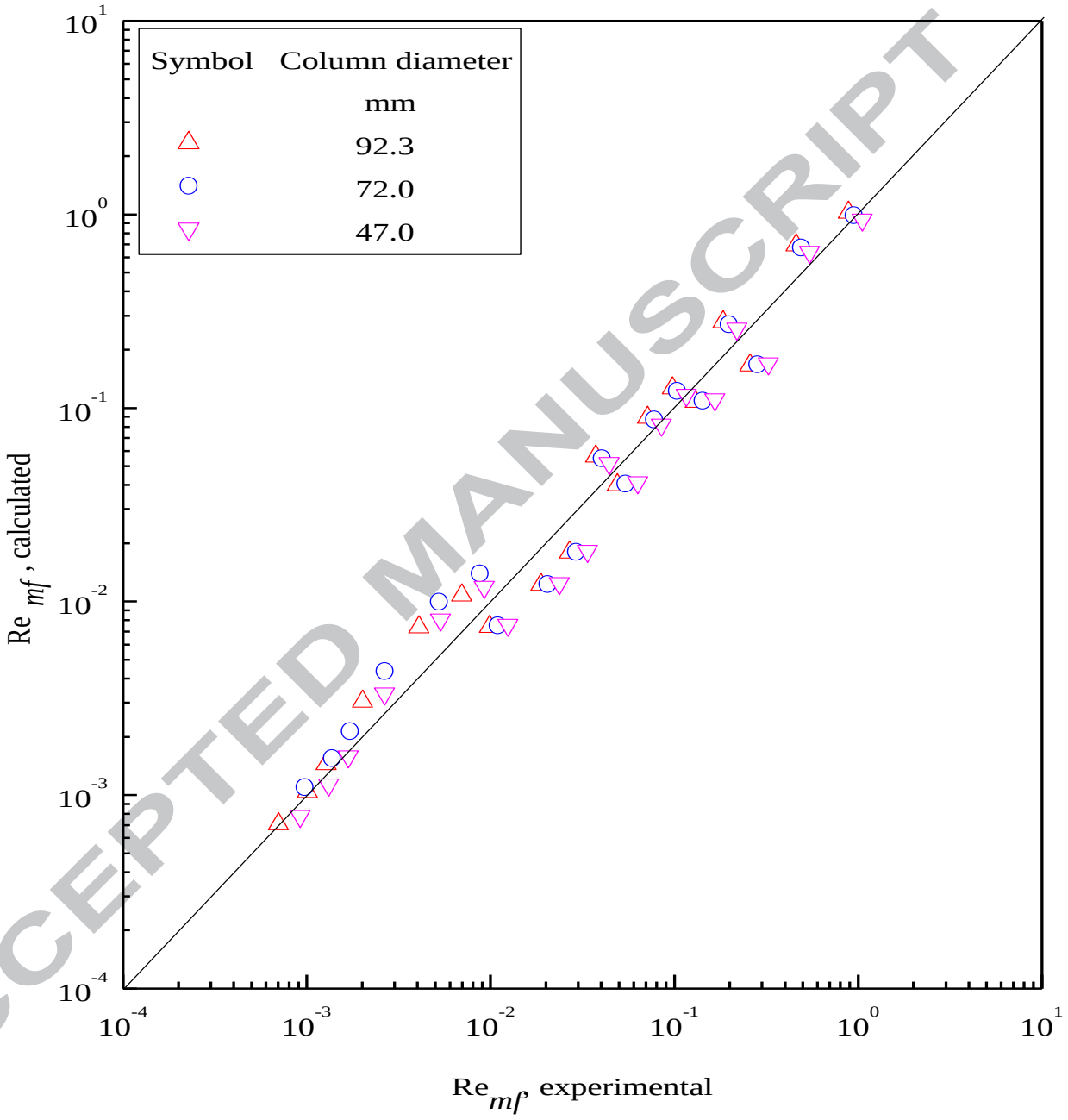

Figure 8

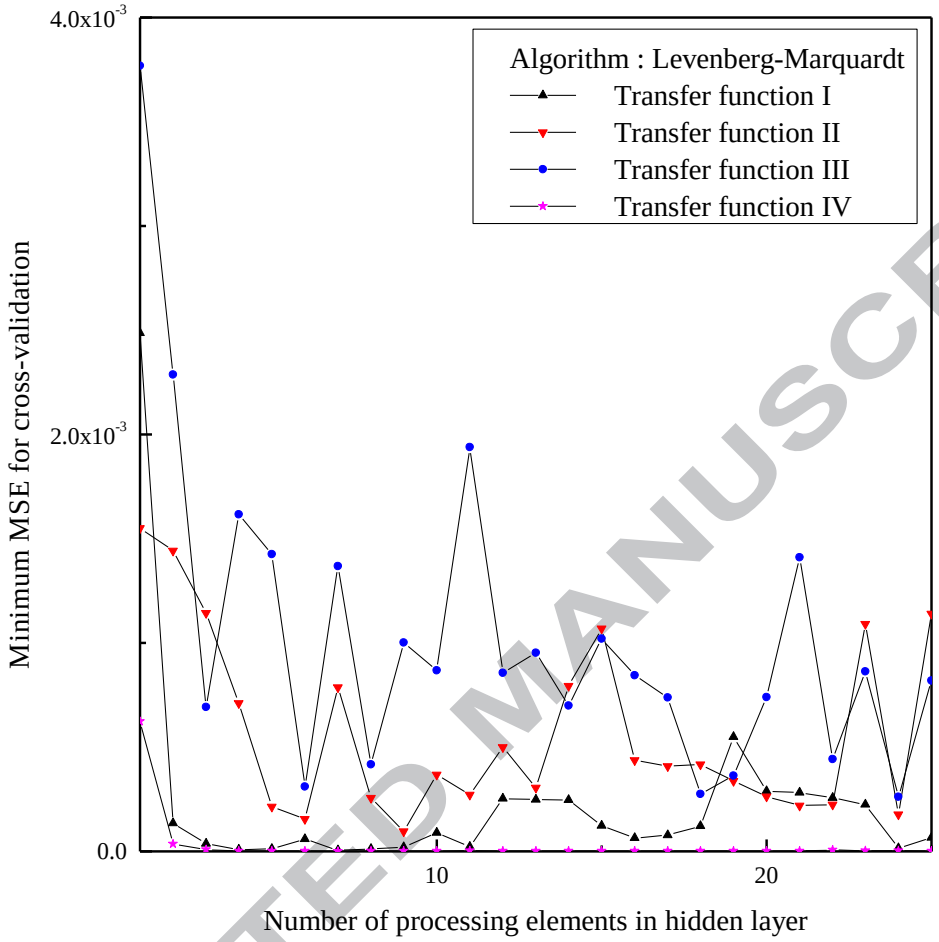

Figure 9

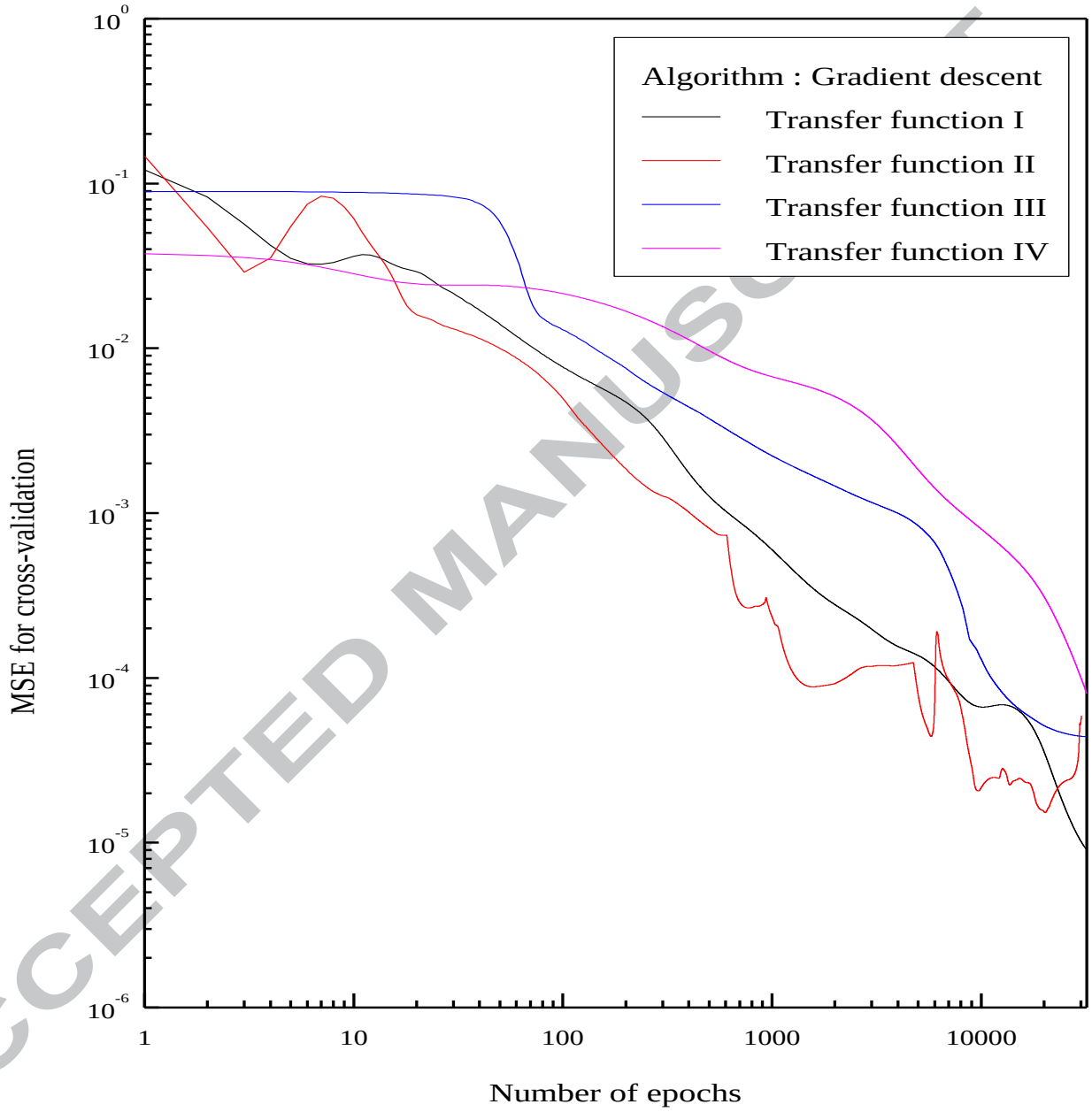

Figure 10

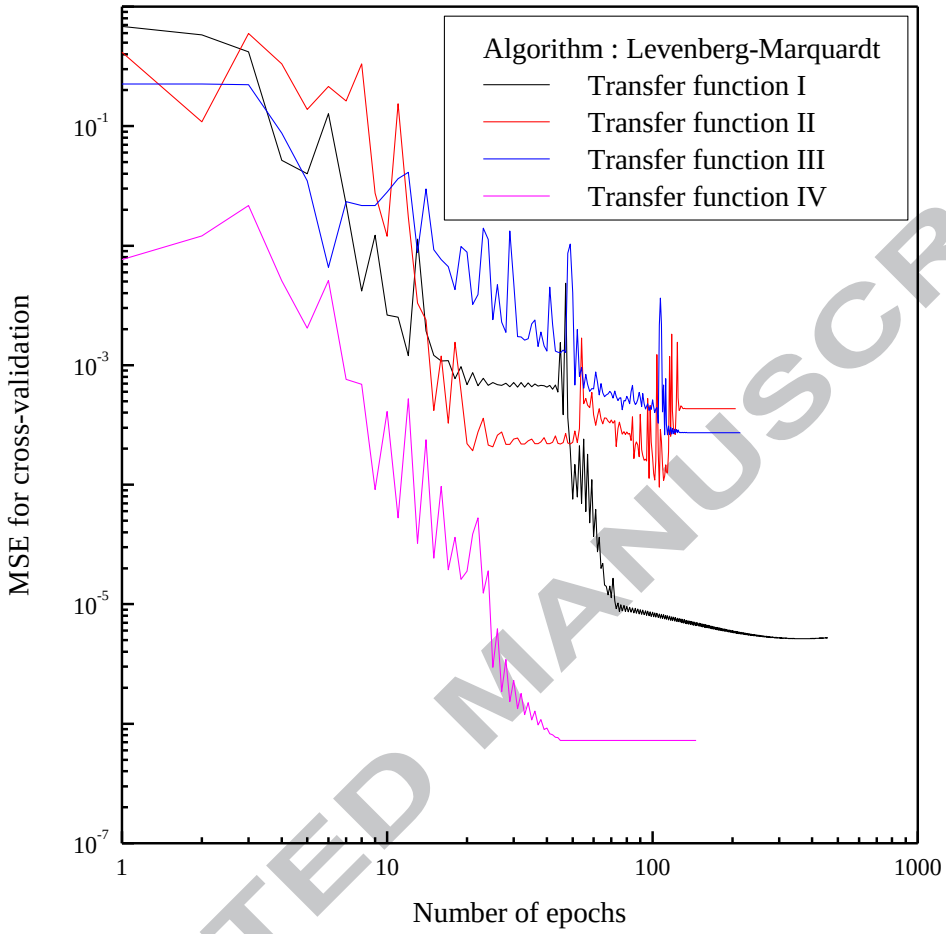

Figure 11

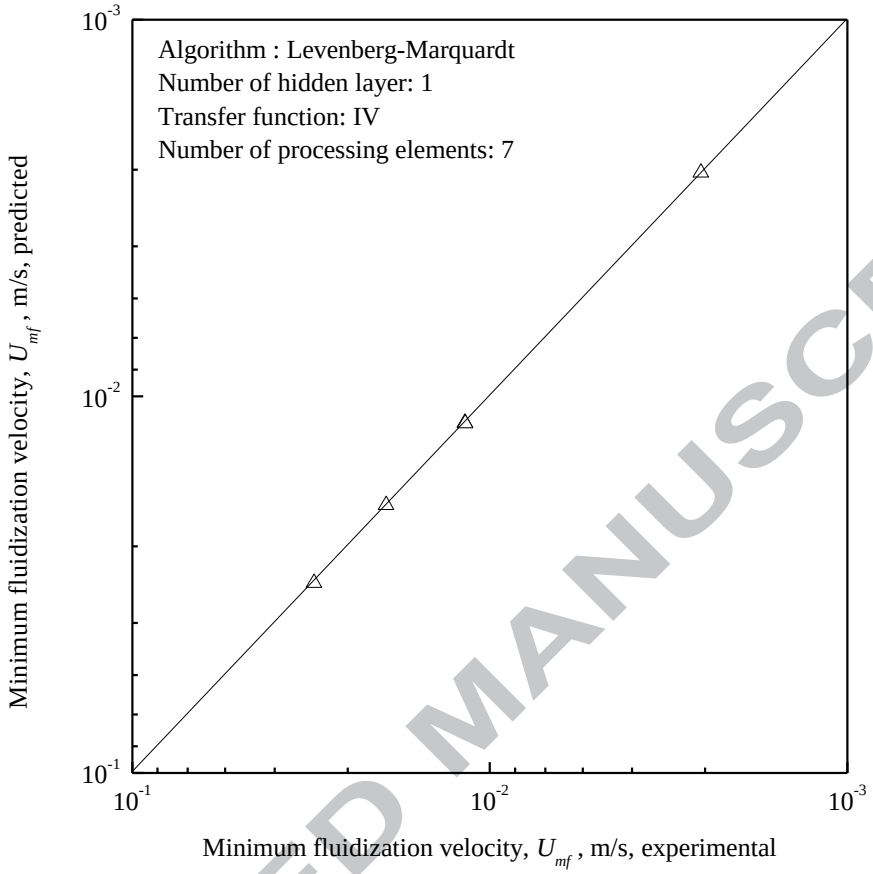

Figure 12

Table 1 Physical property of the sand particle

Particle size mesh	Average particle diameter $d_p \times 10^3$ m	Sphericity ϕ	Particle density ρ_s kg/m^3
-30+36	0.538	0.7965	2650
-25+30	0.651	0.7285	2650
-20+25	0.774	0.6900	2650
-16+20	1.0155	0.5900	2650
-12+16	1.435	0.5610	2650
-8+12	2.03	0.5015	2650

Table 2 Physical properties of the SCMC solutions

Concentration of SCMC kg/m^3	Flow behavior Index n'	Consistency index K' $Ns^{n'}/m^2$	Density ρ_l kg/m^3
0.4	0.7443	0.1222	1002.13
0.6	0.6605	0.3416	1002.87
0.8	0.6015	0.7112	1003.83

Table 3 Range of the experimental data

Measurement type		Range
Input parameters	n'	0.6015 to 0.7443
	K' ($Ns^{n'}/m^2$)	0.1222 to 0.7112
	Density of liquid, ρ_l (kg/m^3)	1002.13 to 1003.83
	Sphericity, ϕ	0.5015 to 0.7965
	Particle diameter, d_p (m)	0.000538 to 0.00203
	Column diameter, d_c (m)	0.047 to 0.0923
Output parameter	Minimum fluidization velocity, U_{mf} (m/s)	0.0019 to 0.039
Total number of data points		54

Table 4 Optimum numbers of processing elements in the hidden layer and the minimum MSE for cross-validation for four different transfer functions

Transfer function in hidden layer	Algorithm	Optimum number of processing elements	minimum MSE for cross-validation
TF I	GD	6	9.057×10^{-6}
	LM	7	5.146×10^{-6}
TF II	GD	6	1.524×10^{-5}
	LM	9	9.558×10^{-5}
TF III	GD	6	4.409×10^{-5}
	LM	24	2.609×10^{-4}
TF IV	GD	3	8.040×10^{-5}
	LM	7	7.251×10^{-7}

Table 5 Performance of the different algorithms for prediction of bed height by the optimized neural network

Transfer function in hidden layer	Measurement type	Algorithm	
		Gradient descent	Levenberg-Marquardt
TF I	AARE	0.016457	0.005211
	SD (σ)	0.012262	0.002569
	MSE	3.18×10^{-8}	2.07×10^{-8}
	CCC (R)	0.999905	0.999945
	χ^2	1.45×10^{-5}	3.74×10^{-6}
TF II	AARE	0.069486	0.046399
	SD (σ)	0.137254	0.022432
	MSE	1.44×10^{-7}	4.46×10^{-7}
	CCC (R)	0.999535	0.998603
	χ^2	3.77×10^{-4}	1.41×10^{-4}
TF III	AARE	0.028462	0.268571
	SD (σ)	0.015389	0.446001
	MSE	1.42×10^{-7}	5.68×10^{-6}
	CCC (R)	0.999284	0.989188
	χ^2	5.28×10^{-5}	–0.045460
TF IV	AARE	0.026649	**0.005155**
	SD (σ)	0.036299	**0.003659**
	MSE	1.49×10^{-7}	$\mathbf{1.59 \times 10^{-8}}$
	CCC (R)	0.999493	**0.999968**
	χ^2	5.69×10^{-5}	$\mathbf{2.95 \times 10^{-6}}$

Table 6 Performance of correlations based on U_{mf}

Method	Correlation	AE (%)
Aghajani et al. (2004)	$\mathrm{Re}_{mf} = \sqrt{(33.7)^2 - 0.0408Ar} - 33.7$	1.31
Eq (7)	$\mathrm{Re}_{mf} = 0.0204Ar^{0.905}(\frac{d_t}{d_p})^{0.589}\phi^{1.300}$	1.998×10^{-3}
ANN	LM algorithm with transfer function TF IV with 7 processing elements in hidden layer	8.168×10^{-3}

Research highlight

- Non-spherical particles were studied in fluidization using non-Newtonian pseudoplastic liquids
- Variation of operating variables were investigated
- Minimum fluidization velocity decreases with decrease with sphericity of the particle
- Empirical correlation to predict the minimum fluidization velocity as a function of physical and dynamic variables of the system were proposed
- Artificial neural network modelling successfully predict the minimum fluidization velocity

Graphical abstract